COBEM 2023 27TH INTERNATIONAL CONGRESS OF MECHANICAL ENGENEERING

ABCM Brazilian Society of Mechanical Sciences and Engineering
27th ABCM International Congress of Mechanical Engineering
December 04-08, 2023, Florianópolis-SC, Brazil

COB-2023-1256
Numerical Simulation of Full-cone Sprays for Liquid Film Formation

Júlio C. A. Ferreira
Marcus V. P. Carneiro
Jader R. Barbosa Jr.
POLO – Research Laboratories for Emerging Technologies in Cooling and Thermophysics, Department of Mechanical Engineering, Federal University of Santa Catarina, Florianópolis – SC, Brazil
jrb@polo.ufsc.br

Abstract. *In this study, we offer a brief overview on full-cone spray modeling. A system of coupled ODEs based on balances of mass, momentum, and energy is used to resolve the spray transport and atomization. An experimental apparatus with a novel 3-colliding jets spray configuration in a vapor-compression refrigeration system is presented in detail. In prior research, we conducted experiments to evaluate spray and jet impingement as cooling schemes for high heat flux applications. The proposed technology integrates the functions of the expansion device and evaporator of a miniaturized, oil-free refrigeration system into a single unit. The two-phase flow inside the cooling unit involves high-pressure subcooled liquid refrigerant entering a jet/spray cooling unit and expanding in one or more orifices, resulting in the formation of either spray or free liquid jets (depending on experimental conditions and setup). These jets then impinge on a heated surface, facilitating convective boiling and evaporation of the liquid film, thereby removing heat. This approach capitalizes on the high heat transfer coefficients of spray and impinging jet, as well as the below-ambient junction temperature of the refrigeration loop. As a result, the compact heat sink has the potential to be applied in numerous vapor-compression cooling systems, including those for power electronics and thermal management of batteries. The full-cone spray model for refrigerant R-134a is compared with different datasets from the literature finding a very good agreement for both the Gaussian droplet velocity radial distribution and the droplet centerline axial velocity away from the injector. The impact velocity is a very important parameter used to determine the liquid film formation and liquid film thickness at the heated surface. Additionally, the full-cone spray model is used for the 3-colliding jets configuration, providing satisfactory results.*

Keywords: *spray cooling, full-cone spray, oil-free compressor, vapor-compression refrigeration system*

1. INTRODUCTION

Direct spray cooling has gained significant interest from the scientific community in recent years due to its effective and dependable performance for electronics thermal management. Various potential applications can be sought when this cooling scheme is integrated into different cooling systems, including vapor-compression refrigeration systems (VCRS) and liquid loops that are powered by pumps. These applications range from high-power electronics (Chen *et al.*, 2022) to aerospace industry (Li *et al.*, 2023) and both conventional and edge data center infrastructure (Kandasamy *et al.*, 2022). The benefit of the VCRS integration with direct spray cooling schemes is, however, twofold, since it combines the high thermal conductance with the ambient temperature independence, a result of below-ambient evaporation temperatures.

Figure 1 illustrates a spray cooling unit of a miniaturized VCRS, detailed elsewhere (Carneiro *et al.*, 2018). High-pressure subcooled liquid from the condenser enters the cooling unit and finds an orifice section where an array of oblique orifices expands the R-134a refrigerant and creates 3 jets oriented to a single point inside the spray chamber. At this point, the two-phase jets collide and atomize in a spray structure that directly impinge on the top of a heated electrolytic copper block, also addressed as heated surface. As the refrigerant droplets impinge on the surface, a thin liquid film may be formed, where different heat transfer mechanisms take place, such as liquid film evaporation, and both single- and two-phase flow convection. Nevertheless, the spray density and thermophysical properties, as well as the droplet size and velocity are some of the key parameters dictating the spray cooling heat transfer performance (Breitenbach *et al.*, 2018).

Therefore, the spray atomization must be properly understood in order to investigate the liquid film formation, flow features, and consequential drying out and flooding limitations. This work focuses on the numerical modeling of the spray atomization for conical sprays, comparing the single injector full-cone sprays with the 3-colliding jets spray configuration from the experiments. This is the first stage in an ongoing work that includes the film formation and evaporation modeling, as well as the spray-film interaction.

2. MODEL

In Lückmann (2010), the author derives an analytical model that resolves the spray droplets for a full-cone spray.

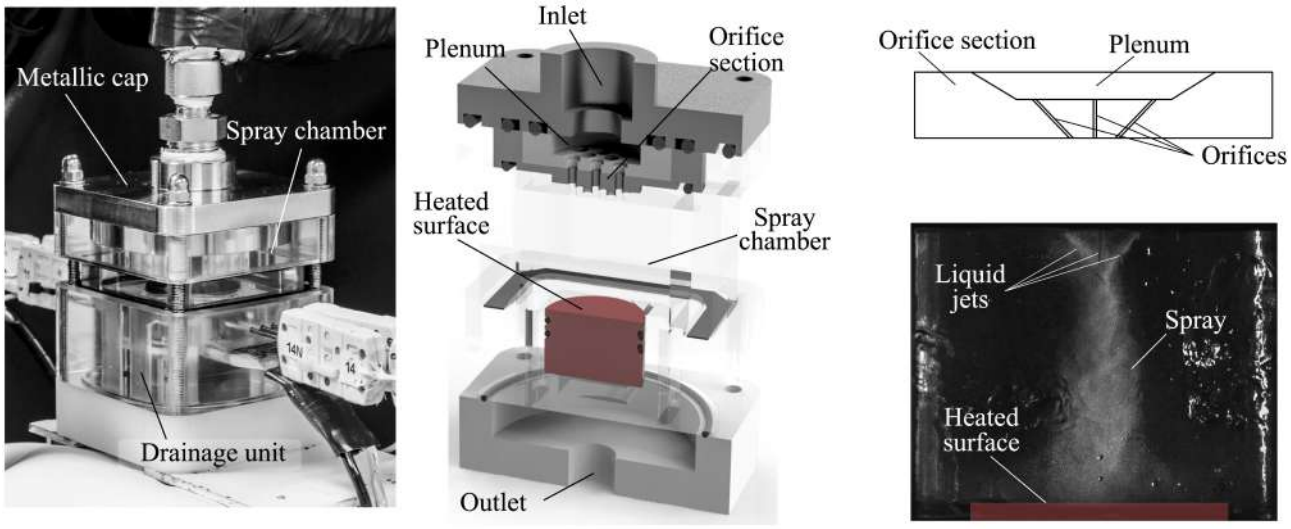

Figure 1. Colliding jet spray configuration. (a) Spray chamber and measurement transducers. (b) CAD model representation of the assembly highlighting the spray chamber and drainage unit. (c) Schematic representation of the colliding jets' orifices and a snapshot of the resulting conical spray.

Assuming a conical profile for the spray with constant angle θ_{spray}, balances of mass, momentum, and energy are applied to an infinitesimal control volume. For simplicity, variations in the angular and radial directions are disregarded, and only the axial direction is considered. Additionally, steady-state, incompressible flow is considered with spherical droplets with no coalescence or break-up. The temperature of the vapor phase is assumed uniform and constant. Figure 2 schematically illustrates the variables overlaid on top of a frame from the experiments.

The domain extends from the injection point to the impinging surface, at axial location $Z_{\max}$. Since the model is 1-D, the variables correspond to the cross-section area-average for any given position z. It is useful to define the fraction of the control-volume occupied by the liquid droplets, the liquid void fraction α_l

$$\alpha_l = \frac{V_d N_d}{\Delta V} \tag{1}$$

where V_d is the droplet volume, N_d the number of droplets in the control volume, and ΔV the volume of the control volume, approximated as $\Delta V = A_{cs}\Delta z$ for small Δz. The cross-section area A_{cs} depends on the cone radius at the given axial position, which can be found from trigonometry, giving

$$A_{cs} = \pi \left[\frac{d_{\text{inj}}}{2} + z \tan\left(\theta_{\text{spray}}/2\right) \right]^2 \tag{2}$$

where d_{inj} is the injection diameter.

The following equations for the liquid void fraction α_l, droplet velocity u_l, vapor velocity u_g and droplet radius r_d can be derived from the mass and momentum balances on the liquid and vapor phases, alongside the energy balance for the droplet liquid-vapor interface [the derivation is presented in detail in Lückmann (2010)]

$$\frac{\mathrm{d}\alpha_l}{\mathrm{d}z} = -\frac{\alpha_l}{u_l}\frac{\mathrm{d}u_l}{\mathrm{d}z} - \frac{3\alpha_l}{r_d}\frac{\dot{m}''_{\text{int}}}{\rho_l u_l} - \frac{2\alpha_l \tan\left(\theta_{\text{spray}}/2\right)}{d_{\text{inj}}/2 + z\tan\left(\theta_{\text{spray}}/2\right)} \tag{3}$$

$$\frac{\mathrm{d}u_l}{\mathrm{d}z} = -\frac{u_l}{2\alpha_l}\frac{\mathrm{d}\alpha_l}{\mathrm{d}z} - \frac{3}{2r_d}\frac{\dot{m}''_{\text{int}}}{\rho_l} - \frac{3}{2r_d}\frac{\tau_{lg}}{\rho_l u_l} - \frac{u_l \tan\left(\theta_{\text{spray}}/2\right)}{d_{\text{inj}}/2 + z\tan\left(\theta_{\text{spray}}/2\right)} \tag{4}$$

$$\frac{\mathrm{d}u_g}{\mathrm{d}z} = \frac{u_g}{2\left(1-\alpha_l\right)}\frac{\mathrm{d}\alpha_l}{\mathrm{d}z} + \frac{3\alpha_l\left(\dot{m}''_{\text{int}}u_l + \tau_{lg}\right)}{2r_d\rho_g\left(1-\alpha_l\right)u_g} - \frac{u_g \tan\left(\theta_{\text{spray}}/2\right)}{d_{\text{inj}}/2 + z\tan\left(\theta_{\text{spray}}/2\right)} \tag{5}$$

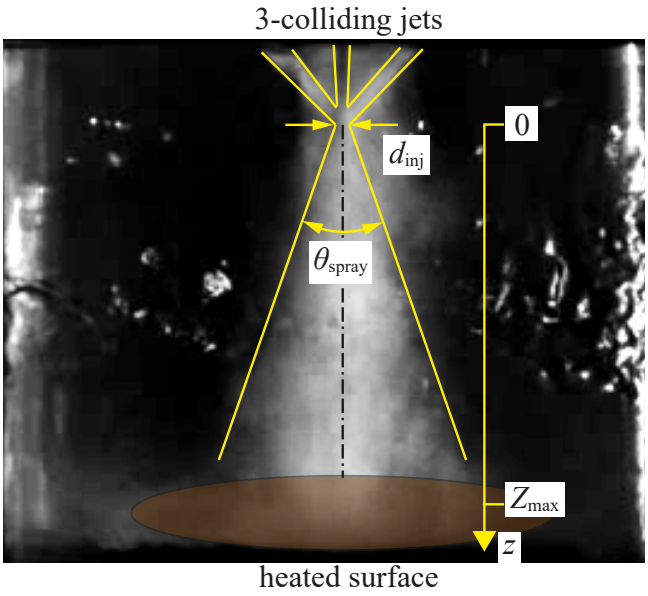

Figure 2. Schematic representation of the spray cone including the injection diameter, spray angle, and distance from the injection point to the heated surface.

$$\frac{\mathrm{d}r_d}{\mathrm{d}z} = -\frac{\dot{m}''_{\text{int}}}{\rho_l u_l} \tag{6}$$

where $\dot{m}''_{\text{int}}$ is the interfacial mass transfer and τ_{lg} is the interfacial shear stress. They are calculated as

$$\dot{m}''_{\text{int}} = -\frac{k_l}{\Delta h_{lg}}\left(\frac{\mathrm{d}T_l}{\mathrm{d}r}\right)_{r=r_d} - \frac{\hbar_d}{\Delta h_l g}\left(T_{l,\text{int}} - T_g\right) \tag{7}$$

$$\tau_{lg} = \frac{1}{8} C_D \rho_l \left(u_l - u_g\right)^2 \tag{8}$$

where $\left(\frac{\mathrm{d}T_l}{\mathrm{d}r}\right)_{r=r_d}$ is the temperature gradient at droplet liquid-vapor interface, obtained from the analytical solution for the temperature distribution in a sphere

$$\left(\frac{\mathrm{d}T_l}{\mathrm{d}r}\right)_{r=r_d} = \frac{2}{r_d}\left(T_{\text{inj}} - T_{lg}\right)\sum_{n} = 1^{\infty}\left[\frac{1}{n\pi}\sin\left(n\pi\right) - \cos\left(n\pi\right)\right]\exp\left(-n^2\pi^2\frac{k_l t}{\rho_l c_{p,l} r_d^2}\right) \tag{9}$$

and $\hbar_d$ and C_D are the droplet heat transfer coefficient and drag coefficient, respectively. Both the heat transfer and the drag coefficients are calculated for a spherical droplet and corrected by the blowing effect (Lefebvre and McDonell, 2017)

$$C_D = C_D^*\left[\frac{B_f}{\exp\left(B_f\right) - 1}\right] = \frac{24}{\text{Re}_d}\left(1 + \frac{\text{Re}_d^{2/3}}{6}\right)\left[\frac{B_f}{\exp\left(B_f\right) - 1}\right] \tag{10}$$

$$\hbar_d = \hbar_d^*\left[\frac{B_h}{\exp\left(B_h\right) - 1}\right] = \frac{k_g \text{Nu}_l}{2r_d}\left[\frac{B_h}{\exp\left(B_h\right) - 1}\right] \tag{11}$$

where B_f and B_h are the blowing correction factor for the shear stress and the heat transfer coefficient, defined as

$$B_f = \frac{8\dot{m}''_{\text{int}}\left|u_l - u_g\right|}{C_D^* \rho_l \left(u_l - u_g\right)^2} \tag{12}$$

Table 1. Experimental conditions for the utilized datasets.

Reference	Fluid	Nozzle	$\dot{m}$, g/s	d_{inj}, µm	θ_{spray}, °	$Z_{\max}$, mm
Hsieh and Tien (2007)	R-134a	Full-cone	0.23–0.26	510	41	90
Zhifu *et al.* (2012)	R-134a	Full-cone	4.3	810	80	200
Chen *et al.* (2019)	R-134a	Full-cone	5.4	800	15	40
Present work	R-134a	3-colliding jets	3.5	500	35-45	20

$$B_h = \frac{2 r_d \dot{m}''_{\mathrm{int}} c_{p,l}}{k_g \mathrm{Nu}_l} \tag{13}$$

and the droplet Reynolds number is defined as $\mathrm{Re}_d = {\rho_g |u_l - u_g| 2 r_d}/{\mu_g}$. The Nusselt number is calculated using the Ranz and Marshall correlation (Ranz and Marshall, 1952)

$$\mathrm{Nu}_l = 2 + 0.6 \mathrm{Re}_d^{1/2} \mathrm{Pr}_g^{1/3} \tag{14}$$

where $\mathrm{Pr}_g = {c_{p,g} \mu_g}/{k_g}$.

The set of Equations (3)-(6) form a system of coupled ODEs that must be solved simultaneously alongside the transport parameters $\dot{m}''_{\mathrm{int}}$, τ_{lg}, and $\hbar_d$. The system is solved numerically using *solve ivp* function from the Python's SciPy module (Virtanen *et al.*, 2020) that uses the Runge-Kutta ODE solver with the implicit Radau method (Hairer and Wanner, 2015).

Two experimental datasets will be used in the validation of the model, namely the R-134a spray velocimetry data from Hsieh and Tien (2007) and Zhifu *et al.* (2012). The adopted experimental conditions are presented in Tab. 1.

Figure 3 shows the axial profiles for the four variables of interest: α_l, u_l, u_g, and r_d using the conditions from Zhifu *et al.* (2012).

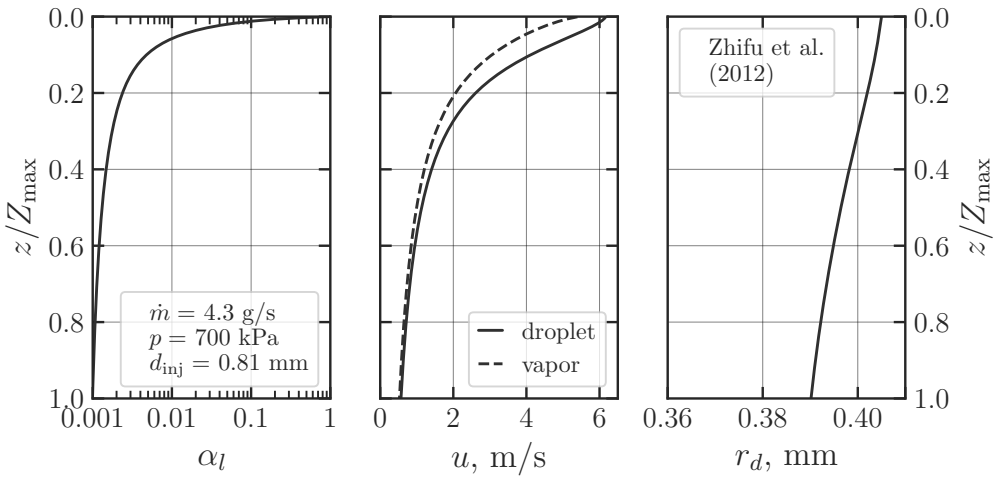

Figure 3. Model results for full-cone nozzle. Data from Zhifu *et al.* (2012)

According to the available literature (Sellens and Brzustowski, 1986; Hsieh and Tien, 2007; Bodaghkhani *et al.*, 2018; Movahednejad *et al.*, 2010; Chen *et al.*, 2019), a Gaussian distribution can be assumed for the droplet velocity as a function of the radial coordinate for each cone section. The droplet velocity radial distribution is then calculated as

$$u_l(r) = \exp\left\{ \left[-\frac{1}{2} \left(\frac{1}{\Omega} \frac{r}{r_{cone}} \right)^2 \right] \right\} u_{l,c} \tag{15}$$

where r_{cone} is the cone section radius and $u_{l,c}$ is the velocity at the spray centerline. The standard deviation is taken as the cone radius multiplied by the factor Ω, taken as 0.15 in the current analysis. The centerline velocity can be found from the definition of the average mass flow rate

$$u_{l,c} = \frac{u_l(r) r_{cone}^2}{2 \int_0^{r_{cone}} r \exp\left\{ \left[-\frac{1}{2} \left(\frac{1}{\Omega} \frac{r}{r_{cone}} \right)^2 \right] \right\} dr} \tag{16}$$

Figure 4 shows a comparison between the velocity distribution obtained from the model for the conditions from Hsieh and Tien (2007). A very good agreement is found for axial locations $z = 40$, 60, and 80 mm, with the first measurement, taken at $z = 20$ mm showing the worst agreement. This result is encouraging since one of the major objectives of the study of this spray is the formation of a liquid film on top of the heated surface, which is strongly dependent on the spray impinging velocity $[u_l(z = Z_{\max})]$, for which the model is well suited.

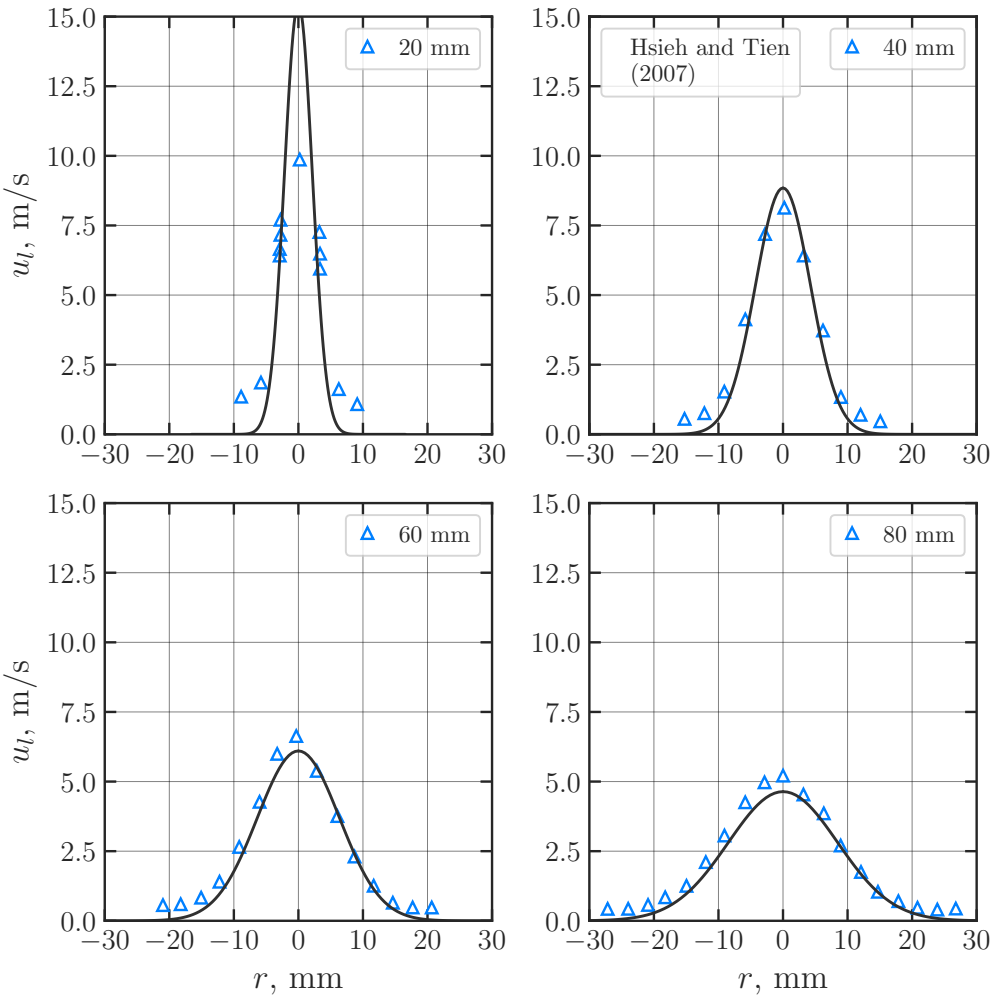

Figure 4. Droplet velocity radial distribution at different axial distances from the injector ($z = 20$, 40, 60, 80 mm). Experimental data from Hsieh and Tien (2007).

Figure 5 shows a direct comparison with experimental data for R-134a sprays from the literature (Hsieh and Tien, 2007; Zhifu *et al.*, 2012; Chen *et al.*, 2019) for the centerline velocity calculated with Eq. (16)

Good agreement is encountered once again for axial locations larger than $z/z_{\max} > 0.2$, showing the suitability of the model in predicting the droplet impact velocity.

3. DISCUSSION OF RESULTS

After the validation for full-cone nozzle sprays, discussed in Section 2, the model from Lückmann (2010) was used to predict the liquid volume fraction, droplet and vapor velocities, and droplet radius for the data from the experimental apparatus described in Section 1 for the 3-colliding jets spray configuration. The relevant parameters are listed in Tab. 1, but special mention is made to the cone angle θ_{spray}, which was manually estimated from isolated frames such as the one displayed in Fig. 2, with encountered values within the range $\theta_{\text{spray}} = 35$-45°.

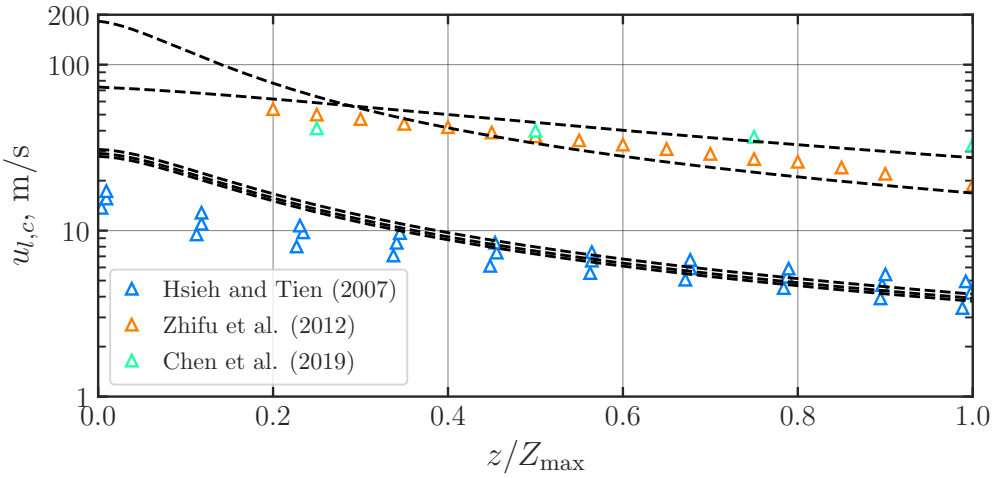

Figure 5. Variation of droplet velocity at the centerline with distance from the injector. Model validation with datasets from Hsieh and Tien (2007); Zhifu *et al.* (2012); Chen *et al.* (2019).

Figure 6 shows the result from the system of ODEs [Eqs. (3)-(6)]. The same overall trend is observed for the 3-colliding jets spray configuration. Due to the shorter distance between the injection point and the heated surface, the droplet radius presents a smaller variation, which results in a larger liquid void fraction at the impact. The cross-section average droplet and vapor velocities show a smoother decay, and the droplet impact cross-section-average velocity can be estimated at around 1 m/s. The uncertainty due to the spray cone angle definition mentioned above is presented as the shaded bands.

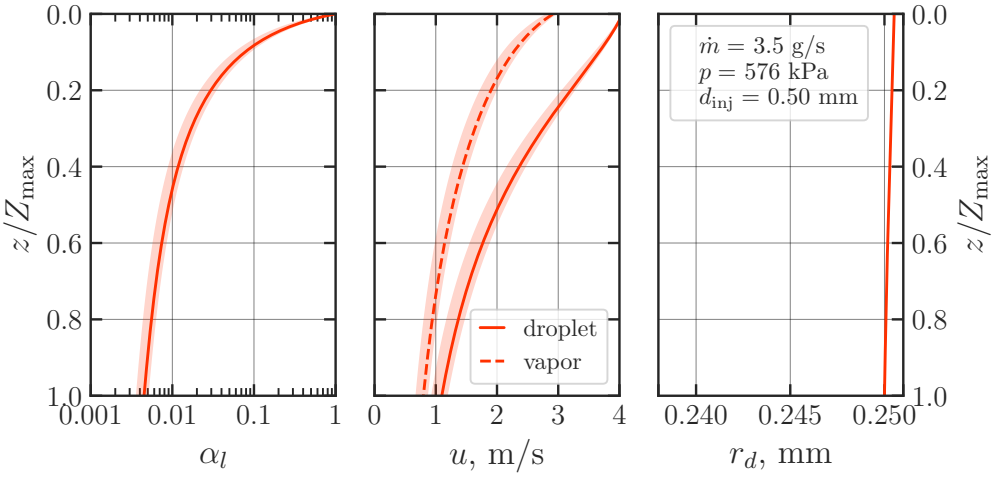

Figure 6. Model results for the 3-colliding jets spray configuration.

Using the Gaussian distribution assumption, the radial droplet velocity profile can be estimated [Eq. (15)], as illustrates Fig. 7. Again, the cone angle uncertainty is presented by the shaded bands.

The Gaussian distribution indicates the droplet impact velocity is much larger at the center, around 30 m/s.

4. CONCLUSIONS

The full-cone spray model developed in Lückmann (2010) was presented and validated with available datasets for R-134a sprays. The droplet radial velocity distribution was found to be satisfactorily predicted by a Gaussian distribution at axial locations farther away from the injection point ($z/Z_{\max} > 0.2$).

The full-cone spray was extended for the 3-colliding jets spray configuration and a similar overall trend was encountered. The impact velocity was estimated from the Gaussian droplet velocity distribution.

Results for the full-cone and 3-colliding jet spray configuration can be fed into a film formation and evaporation model, also discussed in Lückmann (2010), to estimate the heat transfer coefficient.

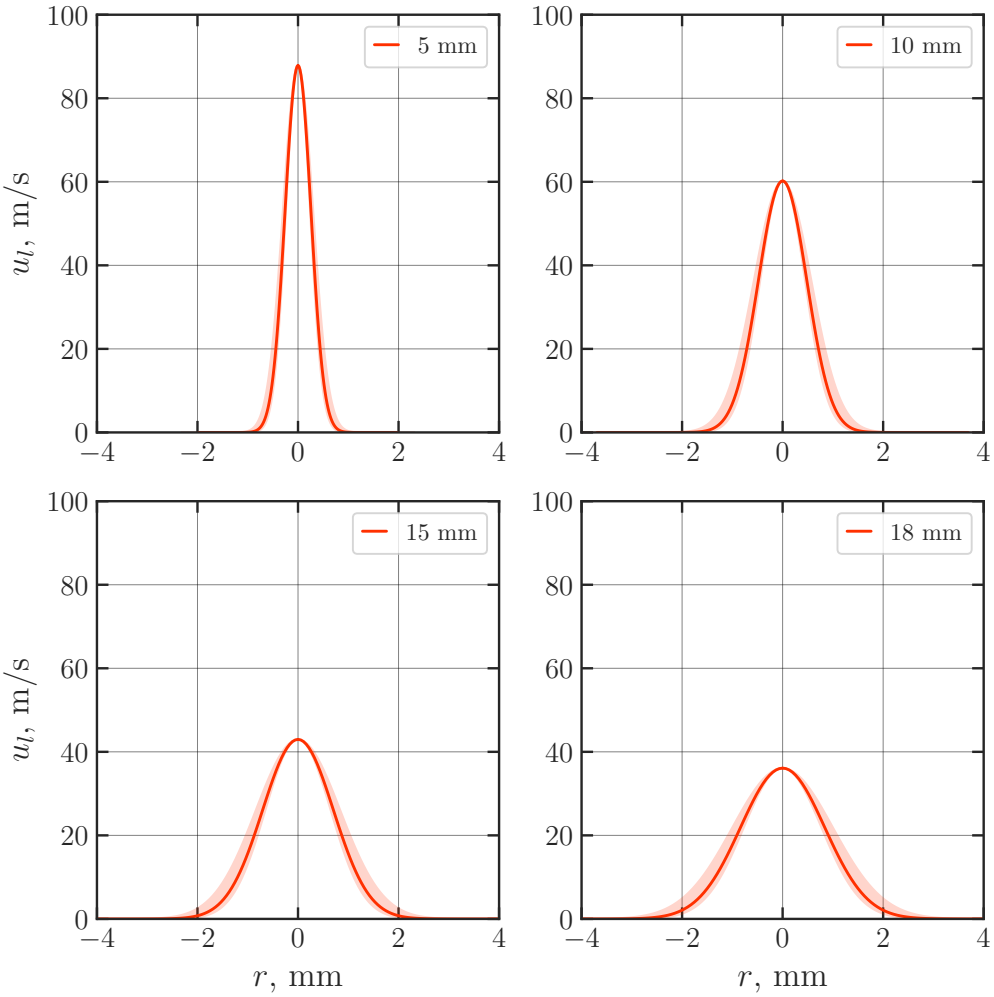

Figure 7. Droplet velocity radial distribution at different axial distances from the injector for the 3-colliding jets spray configuration ($z = 5$, 10, 15, 18 mm).

ACKNOWLEDGEMENTS

Financial support from the National Institute of Science Technology in Cooling and Thermophysics CNPq (Grant No. 404023/2019-3), FAPESC (Grant No. 2019TR0846), EMBRAPII and NIDEC GA (formerly Embraco) is gratefully acknowledged.

REFERENCES

Bodaghkhani, A., Colbourne, B. and Muzychka, Y.S., 2018. "Prediction of droplet size and velocity distribution for spray formation due to wave-body interactions". *Ocean Engineering*, Vol. 155, pp. 106–114. ISSN 0029-8018. doi:https://doi.org/10.1016/j.oceaneng.2018.02.057. URL https://www.sciencedirect.com/science/article/pii/S0029801818302063.

Breitenbach, J., Roisman, I.V. and Tropea, C., 2018. "From drop impact physics to spray cooling models: a critical review". *Experiments in Fluids*, Vol. 59, No. 3, p. 55. doi:10.1007/s00348-018-2514-3.

Carneiro, M.V.P., de Oliveira, P.A. and Barbosa Jr., J.R., 2018. "A compact refrigeration system based on multijet sprays for electronics thermal management". *Experimental Thermal and Fluid Science*, Vol. 97, pp. 180–191.

Chen, B., Tian, J., Wang, R. and Zhou, Z., 2019. "Theoretical study of cryogen spray cooling with r134a, r404a and r1234yf: Comparison and clinical potential application". *Applied Thermal Engineering*, Vol. 148, pp. 1058–1067. ISSN 1359-4311. doi:https://doi.org/10.1016/j.applthermaleng.2018.11.117. URL https://www.sciencedirect.com/science/article/pii/S1359431118353092.

Chen, H., hui Ruan, X., hang Peng, Y., ling Wang, Y. and kun Yu, C., 2022. "Application status and prospect of spray cooling in electronics and energy conversion industries". *Sustainable Energy Technologies and Assessments*, Vol. 52,

p. 102181. ISSN 2213-1388. doi:https://doi.org/10.1016/j.seta.2022.102181.

Hairer, E. and Wanner, G., 2015. *Radau Methods*, Springer Berlin Heidelberg, Berlin, Heidelberg, pp. 1213–1216. ISBN 978-3-540-70529-1. URL https://doi.org/10.1007/978-3-540-70529-1_39.

Hsieh, S.S. and Tien, C.H., 2007. "R-134a spray dynamics and impingement cooling in the non-boiling regime". *International Journal of Heat and Mass Transfer*, Vol. 50, No. 3, pp. 502–512. ISSN 0017-9310. doi:https://doi.org/10.1016/j.ijheatmasstransfer.2006.07.023. URL https://www.sciencedirect.com/science/article/pii/S0017931006004583.

Kandasamy, R., Ho, J.Y., Liu, P., Wong, T.N., Toh, K.C. and Chua, S.J., 2022. "Two-phase spray cooling for high ambient temperature data centers: Evaluation of system performance". *Applied Energy*, Vol. 305, p. 117816. ISSN 0306-2619. doi:https://doi.org/10.1016/j.apenergy.2021.117816.

Lefebvre, A.H. and McDonell, V.G., 2017. *Atomization and Sprays*. CRC Press, 2nd edition. doi: https://doi.org/10.1201/9781315120911.

Li, K., Liu, Z., Xu, J., Liu, H., Xu, S., Wang, C. and Qin, J., 2023. "Evaluation of high-speed aircraft thermal management system based on spray cooling technology: Energy analysis, global cooling, and multi-objective optimization". *Applied Thermal Engineering*, Vol. 229, p. 120632. ISSN 1359-4311. doi: https://doi.org/10.1016/j.applthermaleng.2023.120632.

Lückmann, A.J., 2010. *Modelagem da transferencia de calor com e sem mudanca de fase no resfriamento por spray*. Master's thesis, Universidade Federal de Santa Catarina.

Movahednejad, E., Ommi, F. and Hosseinalipour, S.M., 2010. "Prediction of droplet size and velocity distribution in droplet formation region of liquid spray". *Entropy*, Vol. 12, No. 6, pp. 1484–1498. ISSN 1099-4300. doi: 10.3390/e12061484. URL https://www.mdpi.com/1099-4300/12/6/1484.

Ranz, W.E. and Marshall, W.R., 1952. "Evaporation from drops: Part I". *Chemical Engineering Progress*, Vol. 48, pp. 141–146.

Sellens, R. and Brzustowski, T., 1986. "A simplified prediction of droplet velocity distributions in a spray". *Combustion and Flame*, Vol. 65, No. 3, pp. 273–279. ISSN 0010-2180. doi:https://doi.org/10.1016/0010-2180(86)90041-6. URL https://www.sciencedirect.com/science/article/pii/0010218086900416.

Virtanen, P., Gommers, R., Oliphant, T.E., Haberland, M., Reddy, T., Cournapeau, D., Burovski, E., Peterson, P., Weckesser, W., Bright, J., van der Walt, S.J., Brett, M., Wilson, J., Millman, K.J., Mayorov, N., Nelson, A.R.J., Jones, E., Kern, R., Larson, E., Carey, C.J., Polat, İ., Feng, Y., Moore, E.W., VanderPlas, J., Laxalde, D., Perktold, J., Cimrman, R., Henriksen, I., Quintero, E.A., Harris, C.R., Archibald, A.M., Ribeiro, A.H., Pedregosa, F., van Mulbregt, P. and SciPy 1.0 Contributors, 2020. "SciPy 1.0: Fundamental Algorithms for Scientific Computing in Python". *Nature Methods*, Vol. 17, pp. 261–272. doi:10.1038/s41592-019-0686-2.

Zhifu, Z., Weitao, W., Bin, C., Guoxiang, W. and Liejin, G., 2012. "An experimental study on the spray and thermal characteristics of r134a two-phase flashing spray". *International Journal of Heat and Mass Transfer*, Vol. 55, No. 15, pp. 4460–4468. ISSN 0017-9310. doi:https://doi.org/10.1016/j.ijheatmasstransfer.2012.04.021. URL https://www.sciencedirect.com/science/article/pii/S0017931012002645.

RESPONSIBILITY NOTICE

The authors are solely responsible for the printed material included in this paper.